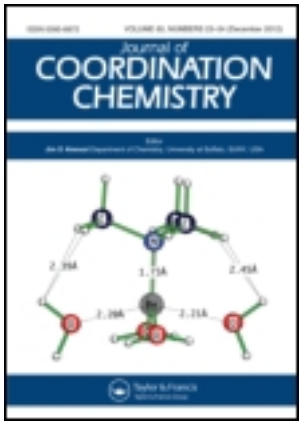

Journal of Coordination Chemistry
Publication details, including instructions for authors and subscription information:
http://www.tandfonline.com/loi/gcoo20

Synthesis, crystal structure, DNA-binding properties, and antioxidant activity of a V-shaped ligand bis(N-methylbenzimidazol-2-ylmethyl)benzylamine and its zinc(II) complex

Huilu Wu [a b], Jingkun Yuan [b], Ying Bai [b], Guolong Pan [b], Hua Wang [b], Juanhui Shao [b], Jiali Gao [b] & Yaoyu Wang [a]

[a] Key Laboratory of Synthetic and Natural Functional Molecule Chemistry of the Ministry of Education, College of Chemistry & Materials Science, Northwest University, Xi'an 710069, P.R. China

[b] School of Chemical and Biological Engineering, Lanzhou Jiaotong University, Lanzhou 730070, P.R. China

Accepted author version posted online: 18 Oct 2012.Published online: 31 Oct 2012.

To cite this article: Huilu Wu, Jingkun Yuan, Ying Bai, Guolong Pan, Hua Wang, Juanhui Shao, Jiali Gao & Yaoyu Wang (2012) Synthesis, crystal structure, DNA-binding properties, and antioxidant activity of a V-shaped ligand bis(N-methylbenzimidazol-2-ylmethyl)benzylamine and its zinc(II) complex, Journal of Coordination Chemistry, 65:24, 4327-4341, DOI: 10.1080/00958972.2012.741229

To link to this article: http://dx.doi.org/10.1080/00958972.2012.741229

Journal of Coordination Chemistry
Vol. 65, No. 24, 20 December 2012, 4327–4341

Synthesis, crystal structure, DNA-binding properties, and antioxidant activity of a V-shaped ligand bis(*N*-methylbenzimidazol-2-ylmethyl)benzylamine and its zinc(II) complex

HUILU WU*†‡, JINGKUN YUAN‡, YING BAI‡, GUOLONG PAN‡, HUA WANG‡, JUANHUI SHAO‡, JIALI GAO‡ and YAOYU WANG†

†Key Laboratory of Synthetic and Natural Functional Molecule Chemistry of the Ministry of Education, College of Chemistry & Materials Science, Northwest University, Xi'an 710069, P.R. China
‡School of Chemical and Biological Engineering, Lanzhou Jiaotong University, Lanzhou 730070, P.R. China

(*Received 25 June 2012; in final form 19 September 2012*)

A V-shaped ligand bis(*N*-methylbenzimidazol-2-ylmethyl)benzylamine (**L**) and its zinc(II) complex, $[Zn\mathbf{L}_2](pic)_2 \cdot 2CH_3CN$ (pic = picrate), have been synthesized and characterized by physico-chemical and spectroscopic methods. Single-crystal X-ray crystallographic analysis revealed that the Zn(II) complex possesses a distorted trigonal bipyramidal geometry. Supramolecular interactions arising from various intra- or intermolecular $\pi\cdots\pi$ stacking interactions contributed to the form of the multidimensional configuration. Interactions of **L** and Zn(II) complex with DNA were monitored using spectrophotometric methods and viscosity measurements. The results suggest that **L** and Zn(II) complex both bind to DNA *via* intercalation and Zn(II) complex binds to DNA more strongly than **L**. Moreover, the Zn(II) complex also exhibited potential antioxidant properties *in vitro*.

Keywords: Benzimidazole; Zinc(II) complex; Crystal structure; DNA-binding property; Antioxidant property

1. Introduction

Transition metal complexes have extensive applications [1–4]. Metal ions present in complexes accelerate drug action and the efficacy of organic therapeutic agents [5]. The pharmacological efficiencies of metal complexes depend on the nature of the metal ions and the ligands [6]; complexes synthesized from same ligands with different metal ions possess different biological properties [5, 7]. There is increasing need for discovery of new compounds having anticancer, antihypertensive, antimicrobial activities, etc. Studies on the mechanism of the interaction of small molecules, such as transition metal complexes, with DNA have been subject of research in bioinorganic and bioorganic

*Corresponding author. Email: wuhuilu@163.com

ISSN 0095-8972 print/ISSN 1029-0389 online
http://dx.doi.org/10.1080/00958972.2012.741229

chemistry [8–11]. Understanding of how these small molecules bind to DNA will potentially be useful in the design of new compounds and reagents, which can recognize specific sites or conformations of DNA [12–14].

Benzimidazole is part of the chemical structure of vitamin B_{12} [15]. Benzimidazoles and their derivatives [16] exhibit a variety of pharmacological activities such as fungicides or anti-helminthics [17]. As a typical heterocyclic ligand, benzimidazole rings can not only provide potential supramolecular recognition sites for $\pi\cdots\pi$ stacking interactions, but also act as hydrogen bond acceptors and donors to assemble multiple coordination geometries [18]. Transition metal complexes containing benzimidazole-based ligands have rich coordination chemistry and a number of established and potential application areas [19, 20].

Our research focuses on transition metal complexes containing benzimidazole-based ligands and exploring the reaction mechanism with DNA [21–27]. In this article, the synthesis, characterization, DNA-binding properties, and antioxidant activity of Zn(II) complex with the V-shaped **L** are presented.

2. Experimental

2.1. *Materials and methods*

All chemicals and solvents were of reagent grade and used without purification. C, H, and N elemental analyses were determined using a Carlo Erba 1106 elemental analyzer. Electrolytic conductance measurements were made with a DDS-307 type conductivity bridge using 3×10^{-3} mol L^{-1} solutions in DMF at room temperature. IR spectra were recorded from 4000 to 400 cm^{-1} with a Nicolet FT-VERTEX 70 spectrometer using KBr pellets. Electronic spectra were taken on a Lab-Tech UV Bluestar spectrophotometer. Fluorescence spectra were performed on an LS-45 spectrofluorophotometer. The absorbance was measured with a Spectrumlab 722sp spectrophotometer at room temperature. ^{1}H-NMR spectra were recorded on a Varian VR300-MHz spectrometer with TMS as an internal standard.

Stock solution of **L** and Zn(II) complex were dissolved in DMF at 3×10^{-3} mol L^{-1}. Calf thymus DNA (*ct*-DNA) and ethidium bromide (EB) were purchased from Sigma. All experiments involving interaction of the ligand and the complexes with *ct*-DNA were carried out in doubly distilled water buffer containing 5 mmol L^{-1} Tris and 50 mmol L^{-1} NaCl and adjusted to pH 7.2 with hydrochloric acid. A solution of *ct*-DNA gave a ratio of UV absorbance at 260 and 280 nm of about 1.8–1.9, indicating that the *ct*-DNA was sufficiently free of protein [28]. The *ct*-DNA concentration per nucleotide was determined spectrophotometrically by employing an extinction coefficient of 6600 (mol L^{-1})$^{-1}$ cm^{-1} at 260 nm [29].

2.2. *Synthesis*

2.2.1. Synthesis of L. **L** was synthesized according to the procedure reported [24]. The synthetic routine of **L** is shown in scheme 1. Yield: 4.85 g (58%); m.p.: 185–186°C. Anal. Calcd for $C_{25}H_{25}N_5$ (%): C, 75.92; H, 6.37; N, 17.71. Found (%): C, 75.69; H, 6.54;

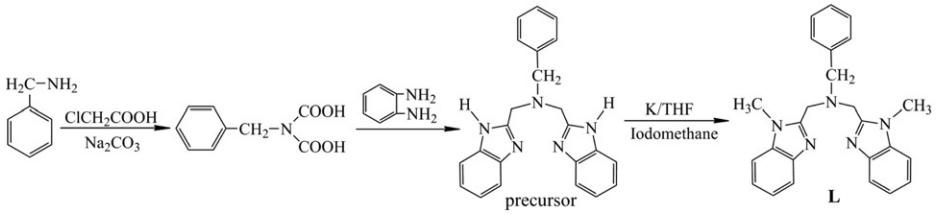

Scheme 1. Synthetic routine of **L**.

N, 17.77. ^{1}H-NMR (DMSO-d$_6$ 400 MHz) δ/ppm: 3.45–3.62 (s, 6H, –CH_3), 3.70 (m, 4H, –CH_2–Ar), 3.90 (m, 4H, –CH_2–benzimidazole), 7.23 (m, 5H, *H*-benzene ring), 7.27–7.61 (m, 8H, *H*-benzimidazole ring). UV-Vis (λ, nm): 279, 287. IR (KBr ν/cm^{-1}): 750, ν(*o*–Ar), 1230, ν(C–N); 1475, ν(C= N); 1616, ν(C=C).

2.2.2. Synthesis of [ZnL$_2$](pic)$_2\cdot$2CH$_3$CN. To a stirred solution of **L** (197.5 mg, 0.50 mmol) in hot EtOH (10 mL) was added Zn(pic)$_2$ (130.40 mg, 0.25 mmol) in EtOH (2 mL). A yellow crystalline product formed rapidly. The precipitate was filtered off, washed with EtOH and absolute Et$_2$O, and dried under vacuum. The crude product was dissolved in MeCN to form a pale yellow solution into which Et$_2$O was allowed to diffuse at room temperature. Yellow crystals suitable for X-ray measurement were obtained after two weeks. Yield: 193.7 mg (72%). Anal. Calcd for $C_{66}H_{62}N_{18}O_{15}Zn$ (%): C, 55.72; H, 4.25; N, 19.69. Found (%): C, 55.95; H, 4.19; N, 19.51. Λ_m(DMF, 297 K): 106.16 S cm^2 mol^{-1}. UV-Vis (λ, nm): 274, 281, 381. FT-IR (KBr ν/cm^{-1}): 746, ν(*o*–Ar); 1263, ν(C–N); 1363, ν(O–N–O); 1490, ν(C= N); 1627, ν(C=C).

Caution: Although no problems are encountered in this work, transition-metal picrate salts are potentially explosive and should thus be prepared in small quantities and handled with care [30].

2.3. *X-ray crystallography*

A suitable single crystal was mounted on a glass fiber and the intensity data were collected on a Bruker Smart CCD diffractometer with graphite-monochromated Mo-Kα radiation ($\lambda = 0.71073$ Å) at 296 K. Data reduction and cell refinement were performed using SMART and SAINT [31]. The structure was solved by direct methods and refined by full-matrix least-squares against F^2 using SHELXTL [32]. All hydrogen atoms were found in difference electron maps and subsequently refined in a riding-model approximation with C–H distances ranging from 0.93 to 0.97 Å and $U_{iso}(H) = 1.2\ U_{eq}(C)$, $U_{iso}(H) = 1.5\ U_{eq}(C_{methyl})$.

2.4. *DNA-binding experiments*

2.4.1. Electronic absorption titration. All spectrophotometric measurements were performed in thermostated quartz sample cells at 25°C. Solutions for analysis were prepared by dilution of stock solutions immediately before the experiments.

Spectrophotometer slit widths were kept at 1 nm for absorption spectroscopy. Electronic absorption titration experiments were performed by maintaining the concentration of the test compounds (ligands/complexes) as constant ($30\,\mu mol\,L^{-1}$) while gradually increasing the concentration of *ct*-DNA. To obtain absorption spectra, the required amount of *ct*-DNA was added to both the compound and reference solutions in order to eliminate the absorbance of *ct*-DNA itself. From the absorption titration data, the binding constant (K_b) was determined using the equation [33]:

$$[DNA]/(\varepsilon_a - \varepsilon_f) = [DNA]/(\varepsilon_b - \varepsilon_f) + 1/K_b(\varepsilon_b - \varepsilon_f),$$

where [DNA] is the concentration of *ct*-DNA in base pairs, ε_a corresponds to the observed extinction coefficient ($A_{obsd}(mol\,L^{-1})^{-1}$), ε_f corresponds to the extinction coefficient of the free compound, ε_b is the extinction coefficient of the compound when fully bound to *ct*-DNA, and K_b is the intrinsic binding constant. The ratio of slope to intercept in the plot of $[DNA]/(\varepsilon_a - \varepsilon_f)$ *versus* [DNA] gave the value of K_b.

2.4.2. Fluorescence studies. Enhanced fluorescence of EB in the presence of DNA can be quenched by addition of a second molecule [34, 35]. The extent of fluorescence quenching of EB bound to *ct*-DNA can be used to determine the extent of binding between the second molecule and *ct*-DNA. Competitive binding experiments were carried out in the buffer by keeping [DNA]/[EB] = 1 and varying the concentrations of the compounds. The fluorescence spectra of EB were measured using an excitation wavelength of 520 nm and the emission range was set between 550 and 750 nm. The influence of the addition of each compound to the DNA–EB complex solution has been obtained by recording the variation of the fluorescence emission spectra. The spectra were analyzed according to the classical Stern–Volmer equation [36]:

$$I_0/I = 1 + K_{SV}[Q],$$

where I_0 and I are the fluorescence intensities at 599 nm in the absence and presence of quencher, respectively, K_{sv} is the linear Stern–Volmer quenching constant, and [Q] is the concentration of the quencher. In these experiments $[ct\text{-DNA}] = 2.5 \times 10^{-3}\,mol\,L^{-1}$, $[EB] = 2.2 \times 10^{-3}\,mol\,L^{-1}$.

2.4.3. Viscosity titration measurements. Viscosity experiments were conducted on an Ubbelodhe viscometer immersed in a water bath maintained at $25.0 \pm 0.1^{\circ}C$. The flow time was measured with a digital stopwatch and each sample was tested three times to get an average calculated time. Titrations were performed for the complexes ($3–30\,\mu mol\,L^{-1}$) and each compound was introduced into *ct*-DNA solution ($42.5\,\mu mol\,L^{-1}$) present in the viscometer. Data were analyzed as $(\eta/\eta_0)^{1/3}$ *versus* the ratio of the concentration of the compound to *ct*-DNA, where η is the viscosity of *ct*-DNA in the presence of the compound and η_0 is the viscosity of *ct*-DNA alone. Viscosity values were calculated from the observed flow time of *ct*-DNA-containing solutions corrected from the flow time of buffer alone (t_0), $\eta = (t - t_0)$ [10].

2.5. *Antioxidant property*

Hydroxyl radicals were generated in aqueous media through the Fenton-type reaction [37, 38]. Aliquots of reaction mixture (3 mL) contained 1.0 mL of 0.10 mmol aqueous safranin, 1 mL of 1.0 mmol aqueous EDTA-Fe(II), 1 mL of 3% aqueous H_2O_2, and a series of quantitative micro-additions of solutions of the test compound. A sample without the tested compound was used as the control. The reaction mixtures were incubated at 37°C for 30 min in a water bath. The absorbance was then measured at 520 nm. All the tests were run in triplicate and are expressed as the mean and standard deviation [39]. The scavenging effect for $OH^{\bullet}$ was calculated from the following expression:

$$\text{Scavenging ratio } (\%) = [(A_i - A_0)/(A_c - A_0)] \times 100\%,$$

where A_i is the absorbance in the presence of the test compound; A_0 is the absorbance of the blank in the absence of the test compound; and A_c is the absorbance in the absence of the test compound, EDTA-Fe(II) and H_2O_2.

3. Results and discussion

L and Zn(II) complex are very stable in air. The Zn(II) complex is remarkably soluble in polar aprotic solvents such as DMF, DMSO, and MeCN; slightly soluble in ethanol, methanol, ethyl acetate, and chloroform; and insoluble in water, Et_2O, and petroleum ether. The molar conductivities in DMF solution indicate that **L** is a nonelectrolyte while the Zn(II) complex is a 1 : 2 electrolyte [40, 41].

3.1. *IR and electronic spectra*

IR spectra of Zn(II) complex are closely related to that of the free **L**. A diagnostic change occurs between 1650 and 1250 cm^{-1}. The spectra of **L** show a strong band at 1475 cm^{-1} and weak band at 1616 cm^{-1}. By analogy with assigned bands of imidazole, the bands are attributed to ν(C=N) and ν(C=C) of the benzimidazole, respectively [42, 43]. The ν(C=N) undergoes a blue-shift (about 15 nm for ν(C=N)) in the Zn(II) complex as compared to the free ligand, indicating direct coordination of two imine nitrogen atoms to metal [44]; these are the preferred nitrogen atoms for coordination, as found in other metal complexes with benzimidazole [45]. Information regarding possible bonding modes of picrate and benzimidazole rings may also be obtained from IR spectra [21, 22].

DMF solutions of **L** and Zn(II) complex show, as expected, almost identical UV spectra. The UV bands of **L** (287, 279 nm) are marginally red-shifted about 5–6 nm for Zn(II) complex, evidence of C=N coordination to the metal center. These bands are assigned to $n \rightarrow \pi^*$ and $\pi \rightarrow \pi^*$ (imidazole) transitions. The picrate bands (observed at 381 nm) are also assigned to $\pi \rightarrow \pi^*$ transitions [23, 24].

Table 1. Crystal data and structure refinement for $[Zn\mathbf{L}_2](pic)_2 \cdot 2CH_3CN$.

Complex	$[Zn\mathbf{L}_2](pic)_2 \cdot 2CH_3CN$
Molecular formula	$C_{66}H_{62}N_{18}O_{15}Zn$
Molecular weight	1412.71
Color	Yellow
Crystal size (mm^3)	$0.34 \times 0.32 \times 0.28$
Crystal system	Triclinic
Space group	$P\bar{1}$
Unit cell dimensions (Å, °)	
a	14.3360(13)
b	15.1189(13)
c	16.1632(14)
α	73.7980(10)
β	82.2770(10)
γ	80.9370(10)
Volume (Å^3), Z	3307.0(5), 2
Temperature (K)	296(2)
Calculated density ($g\,cm^{-3}$)	1.419
$F(000)$	1468
θ range for data collection (°)	1.66–27.54
hkl range	$-18 \le h \le 18$; $-19 \le k \le 19$; $-20 \le l \le 20$
Reflections collected	29,122
Independent reflections	14,900 [$R_{int} = 0.0313$]
Refinement method	Full-matrix least-squares on F^2
Data/restraints/parameters	14,900/17/889
Final R_1/wR_2 indices [$I \ge 2\sigma(I)$][a]	0.0516/0.1300
R_1/wR_2 indices (all data)[a]	0.0789/0.1473
Goodness-of-fit on F^2	1.033
Largest difference peak and hole ($e\,Å^{-3}$)	1.026 and −1.034

[a] $w = 1/[\sigma^2(Fo^2) + (0.0674P)^2 + 2.3587P]$ where $P = (Fo^2 + 2Fc^2)/3$.

Table 2. Selected bond distances (Å) and angles (°).

Complex	$[Zn\mathbf{L}_2](pic)_2 \cdot 2CH_3CN$			
Bond distances	Zn(1)–O(15)	2.02	Zn(1)–N(3)	2.03
	Zn(1)–N(5)	2.02	Zn(1)–N(1)	2.40
	Zn(1)–N(7)	2.02		
Bond angles	O(15)–Zn(1)–N(5)	99.1	N(7)–Zn(1)–N(3)	122.3
	O(15)–Zn(1)–N(7)	94.2	O(15)–Zn(1)–N(1)	172.1
	N(5)–Zn(1)–N(7)	115.5	N(5)–Zn(1)–N(1)	75.8
	O(15)–Zn(1)–N(3)	101.1	N(7)–Zn(1)–N(1)	93.5
	N(5)–Zn(1)–N(3)	116.2	N(3)–Zn(1)–N(1)	76.2

3.2. *X-ray structure of the complex*

Basic crystal data, description of the diffraction experiment, and details of the structure refinement are given in table 1. Selected bond distances and angles are presented in table 2.

The crystal structure of the complex consists of a discrete $[Zn\mathbf{L}_2]^{2+}$, two picrates, and two CH_3CN. The ORTEP (30% probability ellipsoids) of $[Zn\mathbf{L}_2]^{2+}$ with atom-numbering scheme is shown in figure 1.

The Zn(II) is five-coordinate with four nitrogen atoms afforded by two **L** and a H_2O. The coordination geometry of Zn(II) is a distorted trigonal bipyramid with N3, N5, and

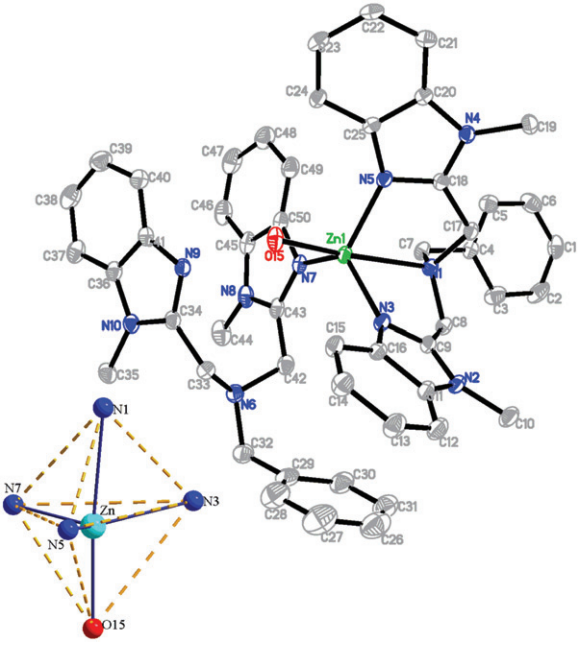

Figure 1. Molecular structure and atom-numbering scheme of $[ZnL_2]^{2+}$ with hydrogen atoms and solvents omitted for clarity.

N7 providing the equatorial plane; Zn(II) is out of this plane by only 0.29 Å. The bond length between the central Zn(II) and three nitrogen atoms forming the equatorial plane are almost equal (average value is 2.03 Å). The distance between Zn–N1 and Zn–O15 are 2.40 and 2.02 Å, respectively. The N1–Zn–O15 bond angle is 172.1°. Therefore, the coordination geometry at Zn(II) can be described as a slightly distorted trigonal bipyramid with a parameter $\tau = 0.83$ [$\tau = (\beta - \alpha)/60$, where α = N(7)–Zn(1)–N(3) = 122.3°, β = O(15)–Zn(1)–N(1) = 172.1°, $\tau = 0$ and 1 for ideal square pyramidal and trigonal bipyramidal geometries, respectively] [46–48].

As shown in figure 2, picrates are inlayed in the coordination cations as a sandwich, held by three types of $\pi\cdots\pi$ stacking interactions [49–52]: (a) between benzimidazole and picrate, $d = 3.65$ Å (d = centroid-to-centroid distance); (b) between two picrates, $d = 3.60$ Å; and (c) between picrate and benzimidazole ring, $d = 3.62$ Å. This provides some groups for formation of hydrogen bonds (table 3), which make the crystal structure more stable. Hence, an infinite 2-D layer is propagated due to the $\pi\cdots\pi$ interactions and hydrogen bonds.

Neighboring layers are connected *via* $\pi\cdots\pi$ stacking interactions ($d = 3.41$ Å), as depicted in figure 3, generating an infinite 3-D network. Supramolecular $\pi\cdots\pi$ stacking interactions may allow the compound to interact with DNA.

3.3. *DNA-binding properties*

3.3.1. Absorption spectroscopic studies. Absorption titration experiments were carried out to investigate binding affinity of **L** and Zn(II) complex with *ct*-DNA. A compound

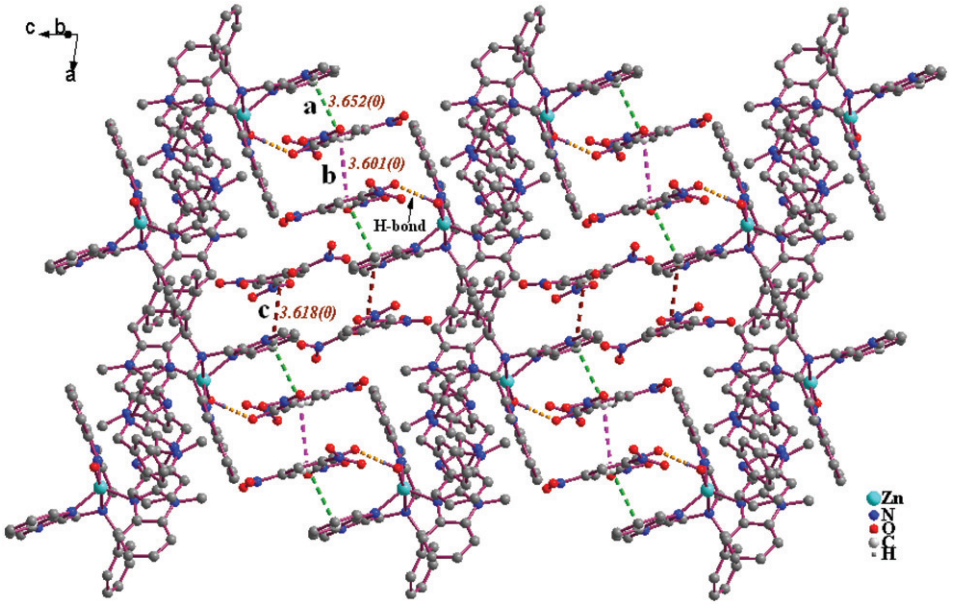

Figure 2. 2-D layer formed *via* $\pi\cdots\pi$ stacking interactions and H-bonds in $[Zn\mathbf{L}_2](pic)_2\cdot 2CH_3CN$; hydrogen atoms and solvent were omitted for clarity.

Table 3. Hydrogen bonds for $[Zn\mathbf{L}_2](pic)_2\cdot 2CH_3CN$ (Å and °).

D–H···A	*d*(D–H)	*d*(H···A)	*d*(D···A)	∠(DHA)
O(15)–H(1W)···N(9)#1	0.83	1.89	2.98	162.8
O(15)–H(2W)···O(1)#1	0.83	1.83	2.65	174.8
C(13)–H(13)···O(8)#1	0.93	2.47	3.34	154.9
C(61)–H(61)···O(13)#1	0.93	2.36	2.68	99.5
C(65)–H(65B)···O(7)#1	0.96	2.50	3.20	129.4
C(1)–H(1)···O(12)#2	0.93	2.59	3.20	123.0
C(5)–H(5)···O(9)#3	0.93	2.52	3.35	148.3
C(8)–H(8A)···O(14)#4	0.97	2.34	3.30	171.6
C(10)–H(10B)···O(3)#4	0.96	2.59	3.42	144.2
C(17)–H(17A)···O(8)#4	0.97	2.58	3.22	124.1
C(19)–H(19C)···O(8)#4	0.96	2.48	3.43	168.7
C(46)–H(46)···O(11)#5	0.93	2.40	3.14	136.4
C(65)–H(65C)···O(13)#6	0.96	2.49	3.45	173.1

Symmetry transformations used to generate equivalent atoms: #1 x, y, z; #2 $x+1, y-1, z$; #3 $x+1, y, z$; #4 $-x+1, -y, -z+1$; #5 $-x+1, -y+1, -z$; #6 $-x+1, -y+1, -z+1$.

binding to DNA through intercalation is characterized by hypochromism in absorbance and red-shift in wavelength due to intercalation involving a strong stacking interaction between the aromatic chromophore and the DNA base pairs [53]. A certain amount of hypochromism is consistent with the strength of the intercalative interaction [54–56]. The electronic spectral traces of **L** and Zn(II) complex titrated with DNA are shown in figure 4. As the DNA concentration increases, the hypochromism reaches 17.30% at 276 nm for free **L**; 38.51% at 272 nm for Zn(II) complex. The λ_{max} for Zn(II) complex

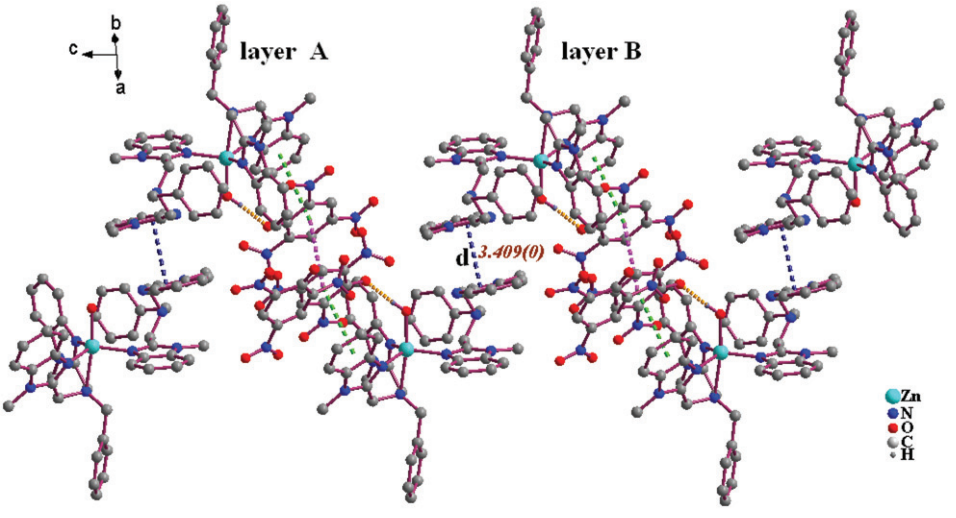

Figure 3. 3-D network formed *via* $\pi\cdots\pi$ stacking interactions in $[ZnL_2](pic)_2\cdot 2CH_3CN$; hydrogen atoms and solvent were omitted for clarity.

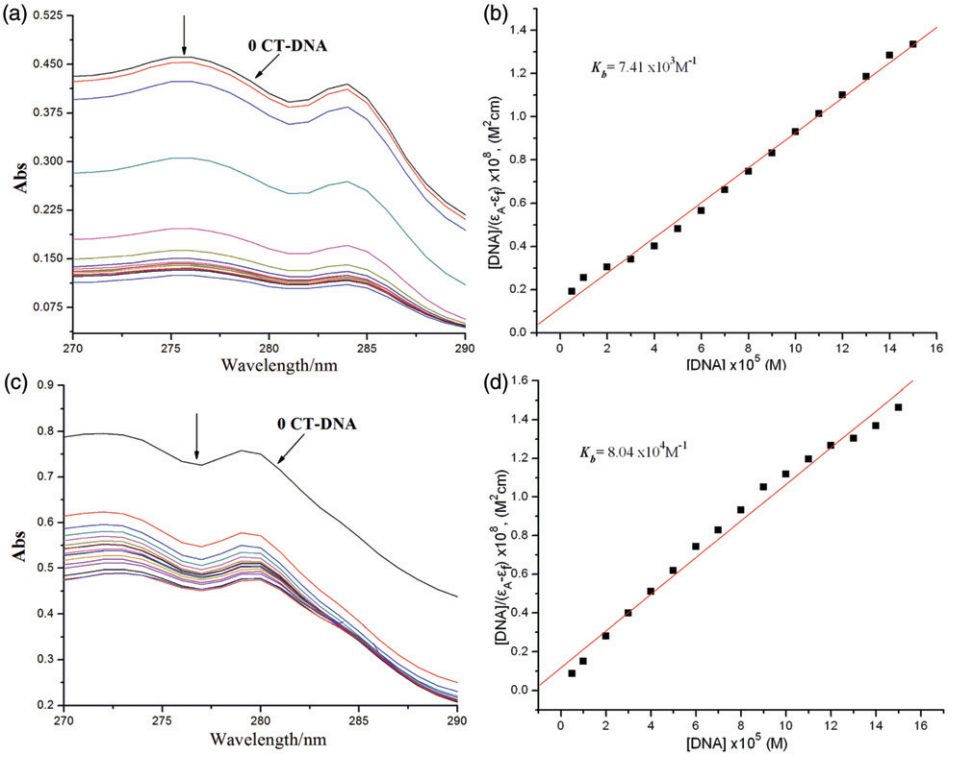

Figure 4. Electronic spectra of (a) **L** and (c) Zn(II) complex in Tris–HCl buffer upon addition of *ct*-DNA. [Compound] = 3×10^{-5} (mol L^{-1})$^{-1}$, [DNA] = 2.5×10^{-5} mol L^{-1}. The arrow shows the emission intensity changes upon increasing DNA concentration. Plots of [DNA]/(ε_a–ε_f) *vs.* [DNA] for the titration of (b) **L** and (d) Zn(II) complex with *ct*-DNA.

increased from 272 to 274 nm, a slight red-shift under identical experimental conditions. The hypochromism suggests that **L** and Zn(II) complex interact with *ct*-DNA, and the spectra also imply that Zn(II) complex binds to DNA more strongly than **L** [57, 58].

To quantitatively compare the affinity toward DNA, the intrinsic binding constants (K_b) of **L** and Zn(II) complex to *ct*-DNA were determined by monitoring the changes of absorbance with increasing concentration of DNA. The K_b of **L** and Zn(II) complex were 7.41×10^3 ($R = 0.99$ for 16 points), 8.04×10^4 $(\text{mol L}^{-1})^{-1}$ ($R = 0.99$ for 16 points), respectively, from the decay of the absorbances. Therefore, compared to classic DNA-intercalative reagents, such as EB, acridine orange, methylene blue [59], and in light of the relevant literature [60–62], the hypochromism and red-shift mentioned above suggest that **L** and Zn(II) bind to DNA with intercalation, due to the large coplanar aromatic rings in **L** and Zn(II) complex that facilitate intercalation to base pairs of double helical DNA.

3.3.2. Fluorescence spectroscopic studies. No luminescence was observed for **L** and Zn(II) complex at room temperature in any organic solvent or in the presence of *ct*-DNA. So the interaction of **L** and Zn(II) complex with *ct*-DNA cannot be directly observed in the emission spectra. Therefore, competitive EB-binding studies were undertaken to examine the binding of each complex with DNA. EB is a conjugate planar molecule. Its fluorescence intensity is very weak, but greatly increased when intercalated into the base pairs of double-stranded DNA [35]. Fluorescence could be quenched by addition of complex which can compete with EB to bind with DNA. This is the proof that complexes intercalate to base pairs of DNA [63].

Fluorescence quenching of DNA-bound EB by **L** and Zn(II) complex are shown in figure 5. The fluorescence intensity of EB-DNA decreases upon addition of **L** and Zn(II) complex. The K_{sv} values for **L** and Zn(II) complex are 1.37×10^4 ($R = 0.99$ for 10 points in the line part) and 2.76×10^4 $(\text{mol L}^{-1})^{-1}$ ($R = 0.99$ for 10 points), respectively, reflecting the higher quenching efficiency of Zn(II) complex relative to that of **L**. This suggests that **L** and Zn(II) complex compete for DNA-binding sites with EB and displace EB from the EB-DNA system [64], characteristic of intercalative interaction of compounds with DNA [65]. Different K_{sv} values indicate that DNA-binding of Zn(II) complex is stronger than that of **L**, consistent with absorption spectral results.

3.3.3. Viscosity titration measurements. Hydrodynamic measurements that are sensitive to length change (i.e., viscosity and sedimentation) are regarded as the least ambiguous and the most critical tests of a binding model in solution in the absence of crystallographic structural data [27, 28, 66]. A classical intercalative molecular interaction causes a significant increase in viscosity of the DNA solution due to increase in separation of the base pairs at the intercalation sites and hence an increase in the overall DNA length [67, 68]. Agents bound to DNA through groove binding do not alter the relative viscosity of DNA, and agents electrostatically bound to DNA will bend or kink the DNA helix, reducing its effective length and its viscosity, concomitantly [66, 69].

Viscosity titration measurements were carried out to clarify the interaction modes between the investigated compounds and *ct*-DNA. The effects of **L** and Zn(II) complex on the viscosity of *ct*-DNA are shown in figure 6. The viscosity of *ct*-DNA increases steadily with increasing amounts, further illustrating intercalation with *ct*-DNA; again

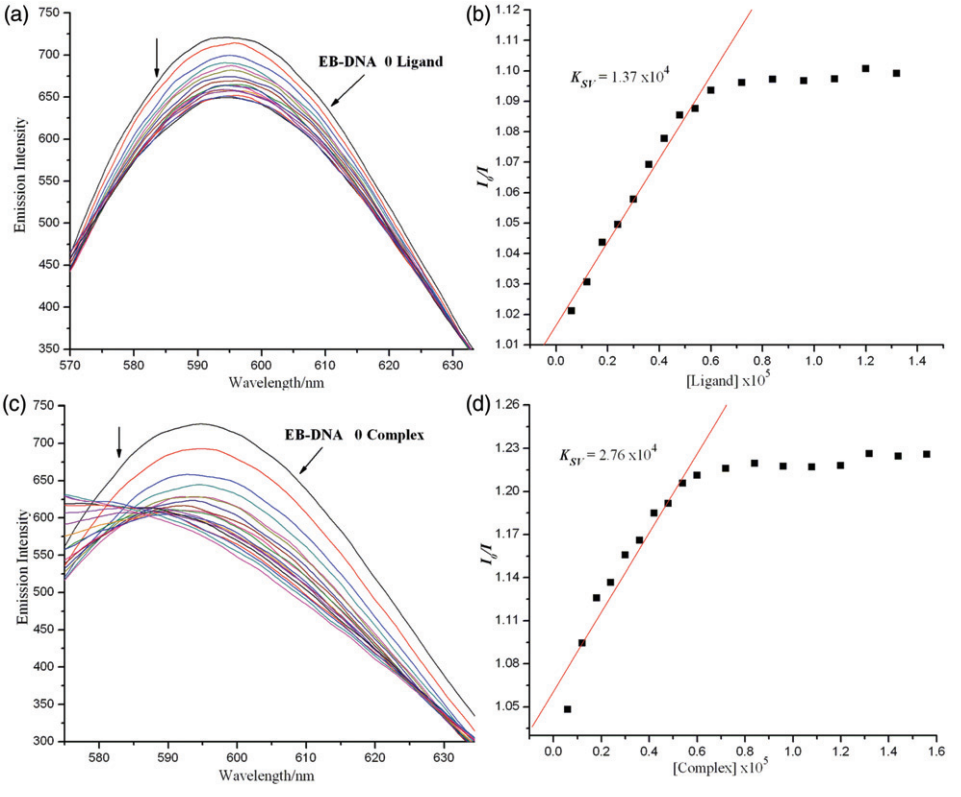

Figure 5. Emission spectra of EB bound to *ct*-DNA in the presence of (a) **L** and (c) Zn(II) complex; [Compound] $= 3 \times 10^{-5}$ mol L^{-1}; $\lambda_{ex} = 520$ nm. The arrows show the intensity changes upon increasing concentrations of the complex. Fluorescence quenching curves of EB bound to *ct*-DNA by (b) **L** and (d) Zn(II) complex (plots of I_0/I *vs.* [Complex]).

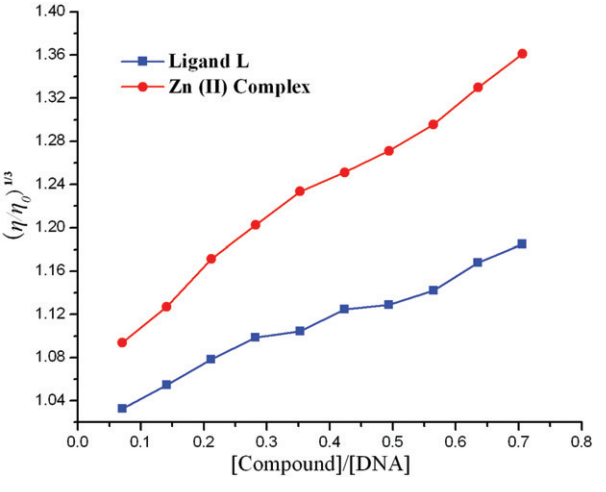

Figure 6. Effect of increasing amounts of **L** and Zn(II) complex on the relative viscosity of *ct*-DNA at 25.0 ± 0.1°C.

the affinity with DNA for Zn(II) complex is stronger than that of **L**. The viscosity experiments confirm **L** and Zn(II) complex intercalation into DNA base pairs already established through absorption and fluorescence spectral titration studies.

The results indicate affinity for DNA is stronger for Zn(II) complex than **L**. Three possible reasons can be used to explain this: (i) the increase in planarity in the compound may lead to higher affinity for DNA, which can be confirmed by the difference between **L** and Zn(II) complex [22, 23], (ii) the charge transfer of coordinated ligands caused by coordination decreases the charge density of the planar conjugate system [70], and (iii) this difference in their DNA-binding ability also could be attributed to the presence of an electron deficient center in the charged Zn(II) complex where an additional interaction between the complex and phosphate rich DNA back bone may occur [71, 72].

3.4. *Antioxidant property*

Since the complexes exhibit reasonable DNA-binding affinity, we also study antioxidant and antiradical activities. Some transition metal complexes display significant antioxidant activity [73–75] and therefore we undertook a systematic investigation on the antioxidant potential of free **L** and Zn(II) complex against $OH^{\bullet}$ radicals with respect to different concentrations of the test compounds.

We compared the abilities to scavenge hydroxyl radicals with those of well-known natural antioxidants mannitol and vitamin C, using the same method as reported [76]. The 50% inhibitory concentration (IC_{50}) value of mannitol and vitamin C are 9.6×10^{-3} and $8.7 \times 10^{-3}\,(\mathrm{mol\,L^{-1}})^{-1}$, respectively. As shown in figure 7, according to the antioxidant experiments, the IC_{50} values of Zn(II) complex is $8.91 \times 10^{-6}\,(\mathrm{mol\,L^{-1}})^{-1}$, which implies that Zn(II) complex has ability to scavenge hydroxyl radical. It can be

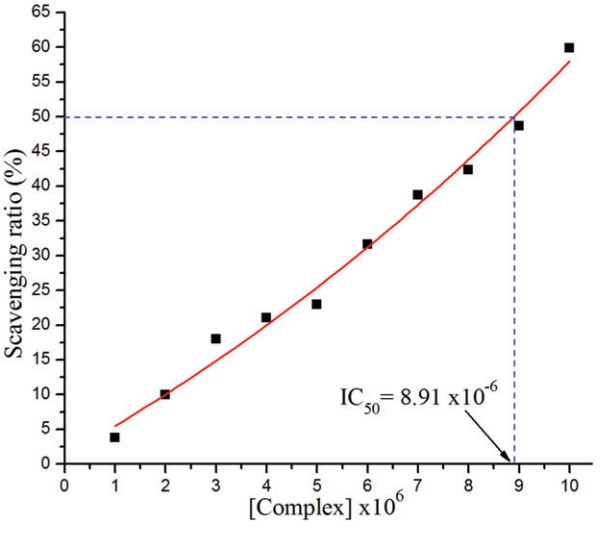

Figure 7. The inhibitory effect of Zn(II) complex on $OH^{\bullet}$ radicals; the suppression ratio increases with increasing concentration of the test compound.

concluded that no scavenging activity was exhibited by **L** when compared to that of Zn(II) complex [77]. The lower IC_{50} values observed in antioxidant assays demonstrate that Zn(II) complex has a strong potential to be applied as scavengers to eliminate the radicals.

4. Conclusion

Bis(*N*-methylbenzimidazol-2-ylmethyl)benzylamine and its Zn(II) complex have been synthesized and characterized. The crystal structure of $[Zn\mathbf{L}_2](pic)_2 \cdot 2CH_3CN$ is a five-coordinate, distorted trigonal bipyramidal geometry. The DNA-binding experiments suggest that **L** and Zn(II) complex can bind to DNA through intercalation, due to the large coplanar aromatic rings in **L** and Zn(II) complex that facilitate intercalation to base pairs of double helical DNA. The Zn(II) complex is stronger than **L**. In addition, the Zn(II) complex can be considered as a potential drug to eliminate hydroxyl radical. The Zn(II) complex has potential practical applications for development of nucleic acid molecular probes and new therapeutic reagents for diseases on the molecular level and warrant further *in vivo* experiments and pharmacological assays.

Supplementary material

Crystallographic data (excluding structure factors) for the structure reported in this article have been deposited with the Cambridge Crystallographic Data Centre with reference number CCDC 853629. Copies of the data can be obtained, free of charge, on application to the CCDC, 12 Union Road, Cambridge CB2 1EZ, UK. Tel: +44-01223-762910; Fax: +44-01223-336033; E-mail: deposit@ccdc.cam.ac.uk or http://www.ccdc.cam.ac.uk.

Acknowledgments

The authors acknowledge the financial support and grant from "Qing Lan" Talent Engineering Funds by Lanzhou Jiaotong University. The grant from "Long Yuan Qing Nian" of Gansu Province also is acknowledged.

References

[1] F. Arjmand, B. Mohani, S. Ahmad. *Eur. J. Med. Chem.*, **40**, 1103 (2005).
[2] S. Parveen, F. Arjmand, S. Parveen, F. Arjmand. *Spectrochim. Acta, Part A*, **85**, 53 (2012).
[3] E.L. Hegg, J.N. Burstyn. *Coord. Chem. Rev.*, **173**, 133 (1998).
[4] L.J.K. Boerner, J.M. Zaleski. *Curr. Opin. Chem. Biol.*, **9**, 135 (2005).
[5] Z.A. Siddiqi, M. Khalid, S. Kumar, M. Shahid, S. Noor. *Eur. J. Med. Chem.*, **45**, 264 (2010).
[6] S. Delaney, M. Pascaly, P.K. Bhattacharya, K. Han, J.K. Barton. *Inorg. Chem.*, **41**, 1966 (2002).
[7] K. Serbest, A. Colak, S. Güner, S. Karaböcek. *Trans. Met. Chem.*, **26**, 625 (2001).

[8] Y.M. Song, Q. Wu, P.J. Yang, N.N. Luan, L.F. Wang, Y.M. Liu. *J. Inorg. Biochem.*, **100**, 1685 (2006).
[9] J. Tan, B. Wang, L. Zhu. *Bioorg. Med. Chem.*, **17**, 614 (2009).
[10] C.P. Tan, J. Liu, L.M. Chen, S. Shi, L.N. Ji. *J. Inorg. Biochem.*, **102**, 1644 (2008).
[11] S. Gopal, U.N. Balachandran. *Eur. J. Med. Chem.*, **45**, 284 (2010).
[12] K.E. Erkkila, D.T. Odom, J.K. Barton. *Chem. Rev.*, **99**, 2777 (1999).
[13] L.N. Ji, X.H. Zou, J.G. Lin. *Coord. Chem. Rev.*, **216–217**, 513 (2001).
[14] B.M. Zeglis, V.C. Pierre, J.K. Barton. *Chem. Commun.*, 4565 (2007).
[15] J.B. Wright. *Chem. Rev.*, **48**, 397 (1951).
[16] D.A. Horton, G.T. Bourne, M.L. Smythe. *Chem. Rev.*, **103**, 893 (2003).
[17] T.M. Aminabhavi, N.S. Biradar, S.B. Patil, D.E. Hoffman. *Inorg. Chim. Acta*, **125**, 125 (1986).
[18] H.Y. Liu, H. Wu, J. Yang, Y.Y. Liu, B. Liu, Y.Y. Liu, J.F. Ma. *Cryst. Growth Des.*, **11**, 2920 (2011).
[19] J.A. Cowan. *Chem. Rev.*, **98**, 1067 (1998).
[20] C.L. Liu, M. Wang, T.L. Zhang, H.Z. Sun. *Coord. Chem. Rev.*, **248**, 147 (2004).
[21] H.L. Wu, X.C. Huang, J.K. Yuan, F. Kou, F. Jia, B. Liu, K.T. Wang. *Eur. J. Med. Chem.*, **45**, 5324 (2010).
[22] H.L. Wu, J.K. Yuan, Y. Bai, G.L. Pan, H. Wang, X.B. Shu. *J. Photochem. Photobiol. B*, **107**, 65 (2012).
[23] H.L. Wu, J.K. Yuan, Y. Bai, F. Jia, B. Liu, F. Kou, J. Kong. *Trans. Met. Chem.*, **36**, 819 (2011).
[24] H.L. Wu, J.K. Yuan, Y. Bai, G.L. Pan, H. Wang, X.B. Shu, G.Q. Yu. *J. Coord. Chem.*, **65**, 616 (2012).
[25] H.L. Wu, K.T. Wang, F. Kou, F. Jia, B. Liu, J.K. Yuan, Y. Bai. *J. Coord. Chem.*, **64**, 2676 (2011).
[26] H.L. Wu, X.C. Huang, B. Liu, F. Kou, F. Jia, J.K. Yuan, Y. Bai. *J. Coord. Chem.*, **64**, 4383 (2011).
[27] H.L. Wu, T. Sun, K. Li, B. Liu, F. Kou, F. Jia, J.K. Yuan, Y. Bai. *Bioinorg. Chem. Appl.*, **2012**, 609796 (2012).
[28] S. Satyanarayana, J.C. Dabrowiak, J.B. Chaires. *Biochemistry*, **32**, 2573 (1993).
[29] M.E. Reichmann, S.A. Rice, C.A. Thomas, P. Doty. *J. Am. Chem. Soc.*, **76**, 3047 (1954).
[30] D.G. Churchill. *J. Chem. Educ.*, **83**, 1798 (2006).
[31] Bruker. *SMART, SAINT and SADABS*, Bruker Axs, Inc., Madison, WI (2000).
[32] G.M. Sheldrick. *SHELXTL*, Siemens Analytical X-ray Instruments, Inc., Madison, WI (1996).
[33] A.M. Pyle, J.P. Rehmann, R. Meshoyrer, C.V. Kumar, N.J. Turro, J.K. Barton. *J. Am. Chem. Soc.*, **111**, 3051 (1989).
[34] A. Wolf, G.H. Shimer, T. Meehan. *Biochemistry*, **26**, 6392 (1987).
[35] B.C. Baguley, M.L. Bret. *Biochemistry*, **23**, 937 (1984).
[36] J.R. Lakowicz, G. Webber. *Biochemistry*, **12**, 4161 (1973).
[37] C.C. Winterbourn. *Biochem. J.*, **198**, 125 (1981).
[38] C.C. Winterbourn. *Biochem. J.*, **182**, 625 (1979).
[39] Z.Y. Guo, R.E. Xing, S. Liu, H.H. Yu, P.B. Wang, C.P. Li, P.C. Li. *Bioorg. Med. Chem. Lett.*, **15**, 4600 (2005).
[40] W.J. Geary. *Coord. Chem. Rev.*, **7**, 81 (1971).
[41] W.K. Dong, J.G. Duan. *J. Coord. Chem.*, **61**, 781 (2008).
[42] N.M. Aghatabay, B. Dulger, F. Gucin. *Eur. J. Med. Chem.*, **40**, 1096 (2005).
[43] N.M. Aghatabay, M. Tulu, Y. Mahmiani, M. Somer, B. Dulger. *Struct. Chem.*, **19**, 71 (2008).
[44] C.Y. Su, B.S. Kang, C.X. Du, Q.C. Yang. *Inorg. Chem.*, **39**, 4843 (2000).
[45] K. Nakamoto. *Infrared and Raman Spectra of Inorganic and Coordination Compounds*, 3rd Edn, pp. 200–320, John Wiley and Sons, New York (1978).
[46] A.W. Addison, T.N. Rao, J. Reedijk, J. Van Rijn, G.C. Verschoor. *J. Chem. Soc., Dalton Trans.*, 1349 (1984).
[47] M. Bröring, C.D. Brandt. *Chem. Commun.*, 2156 (2003).
[48] R.B. Bedford, M. Betham, C.P. Butts, S.J. Coles, M. Cutajar, T. Gelbrich, M.B. Hursthouse, P.N. Scullyd, S. Wimperisc. *Dalton Trans.*, 459 (2007).
[49] K.N. Power, T.L. Hennigar, M.J. Zaworotko. *New J. Chem.*, **22**, 177 (1998).
[50] O.M. Yaghi, H.J. Li. *J. Am. Chem. Soc.*, **118**, 295 (1996).
[51] C.L. Chen, C.Y. Su, Y.P. Cai, H.X. Zhang, A.W. Xu, B.S. Kang, Z.L. Hans-Conrad. *Inorg. Chem.*, **42**, 3738 (2003).
[52] W.K. Dong, Y.X. Sun, C.Y. Zhao, X.Y. Dong, L. Xu. *Polyhedron*, **29**, 2087 (2010).
[53] M. Baldini, M. Belicchi-Ferrari, F. Bisceglie, P.P. Dall'Aglio, G. Pelosi, S. Pinelli, P. Tarasconi. *Inorg. Chem.*, **43**, 7170 (2004).
[54] J.K. Barton, A.T. Danishefsky, J.M. Goldberg. *J. Am. Chem. Soc.*, **106**, 2172 (1984).
[55] S.A. Tysoe, R.J. Morgan, A.D. Baker, T.C. Strekas. *J. Phys. Chem.*, **97**, 1707 (1993).
[56] J.M. Kelly, A.B. Tossi, D.J. McConnell, C. OhUigin. *Nucleic Acids Res.*, **13**, 6017 (1985).
[57] J. Liu, T.X. Zhang, L.N. Ji. *J. Inorg. Biochem.*, **91**, 269 (2002).
[58] H. Xu, K.C. Zheng, Y. Chen, Y.Z. Li, L.J. Lin, H. Li, P.X. Zhang, L.N. Ji. *Dalton Trans.*, 2260 (2003).
[59] S. Nafisi, A.A. Saboury, N. Keramat, J.F. Neault, H.A. Tajmir-Riahi. *J. Mol. Struct.*, **827**, 35 (2007).
[60] K. Pothiraj, T. Baskaran, N. Raman. *J. Coord. Chem.*, **65**, 2110 (2012).
[61] A.K. Asatkar, S. Nair, V.K. Verma, C.S. Verma, T.A. Jain, R. Singh, S.K. Gupta, R.J. Butcher. *J. Coord. Chem.*, **65**, 28 (2012).

[62] N. Raman, K. Pothiraj, T. Baskaran. *J. Coord. Chem.*, **64**, 3900 (2011).
[63] Q. Wang, Z.Y. Yang, G.F. Qi, D.D. Qin. *Eur. J. Med. Chem.*, **44**, 2425 (2009).
[64] Y.B. Zeng, N. Yang, W.S. Liu, N. Tang. *J. Inorg. Biochem.*, **97**, 258 (2003).
[65] C.V. Kumar, J.K. Barton, N.J. Turro. *J. Am. Chem. Soc.*, **107**, 5518 (1985).
[66] S. Satyanarayana, J.C. Dabroniak, J.B. Chaires. *Biochemistry*, **31**, 9319 (1992).
[67] D. Suh, J.B. Chaires. *Bioorg. Med. Chem.*, **3**, 723 (1995).
[68] R. Palchaudhuri, P.J. Hergenrother. *Curr. Opin. Biotechnol.*, **18**, 497 (2007).
[69] B.D. Wang, Z.Y. Yang, P. Crewdson, D.Q. Wang. *J. Inorg. Biochem.*, **101**, 1492 (2007).
[70] T. Ihara, S. Sueda, A. Inenaga, R. Fukuda, M. Takagi. *Supramol. Chem.*, **8**, 93 (1997).
[71] S. Yellappa, J. Seetharamappa, L.M. Rogers, R. Chitta, R.P. Singhal, F. D'Souza. *Bioconjugate Chem.*, **17**, 1418 (2006).
[72] M. Shakir, M. Azam, M.F. Ullah, S.M. Hadi. *J. Photochem. Photobiol. B*, **104**, 449 (2011).
[73] S.B. Bukhari, S. Memon, M. Mahroof-Tahir, M.I. Bhanger. *Spectrochim. Acta, Part A*, **71**, 1901 (2009).
[74] F.V. Botelho, J.I. Alvarez-Leite, V.S. Lemos, A.M.C. Pimenta, H.D.R. Calado, T. Matencio, C.T. Miranda, E.C. Pereira-Maia. *J. Inorg. Biochem.*, **101**, 935 (2007).
[75] Q. Wang, Z.Y. Yang, G.F. Qi, D.D. Qin. *Eur. J. Med. Chem.*, **44**, 2425 (2009).
[76] T.R. Li, Z.Y. Yang, B.D. Wang, D.D. Qin. *Eur. J. Med. Chem.*, **43**, 1688 (2008).
[77] J.I. Ueda, N. Saito, Y. Shimazu, T. Ozawa. *Arch. Biochem. Biophys.*, **333**, 377 (1996).